Study of different tyre simulation methods and effects on passenger car aerodynamics

Study of different tyre simulation methods and effects on passenger car aerodynamics

T. Hobeika, L. Löfdahl *
S. Sebben **

***Applied Mechanics, Chalmers University of Technology, Sweden**
****Volvo Car Corporation, Sweden**

ABSTRACT

Wheel aerodynamics has long been identified as a major contributor to the aerodynamic forces acting on vehicles. Lately, tyre design has been taking more and more attention as it shows potential of drag reduction. This paper looks into different methods of simulating tyre rotations in CFD and their effects on the aerodynamic forces acting on the vehicle. A new methodology is tested by combining rotating wall and moving reference frame boundary conditions and compared to sliding mesh. Two fully detailed production tyres are investigated using the various methods to show the possibility of tyre design analysis using CFD.

1 INTRODUCTION

During the last several years, wheel aerodynamics has been the focus of several projects and investigations for better understanding of their influence on the flow field around passenger vehicles and its effect on aerodynamic forces (1; 2; 3). Wheel aerodynamics in general has shown to be quite a complex phenomenon presenting many challenges to researchers. Although the wheel is split into tyre and rim, the aerodynamic effects of each cannot be easily separated as they seem to interact together to a large extent. The understanding of the aerodynamic effects these two components can be key in optimizing low drag rim and tyre designs for future road vehicles while also reducing road load through ventilation drag (4; 5; 6; 7; 8; 9).

On average the car development takes around 4 to 5 years, with aerodynamicists engaging quite early in the design process of the vehicle to reach the target drag and lift coefficients. This usually relies heavily on CFD simulations in the early phases of the project until it becomes possible to produce and test clay models in wind tunnels. However even when clay models are produced for wind tunnel testing, the tyres and rims to be mounted on the car usually come into production very late into the project. This adds a significant uncertainty to the predictions and could lead to inappropriate vehicle optimizations in certain areas around the underbody of the car where the wheels have a large effect on the flow. For this reason it is important to be able to use CFD simulations to predict the aerodynamic effects of the rims and tyres. This will not only lead to identifying key areas which are influenced by these parts, but also the optimization of the tyre and rims can be performed for the specific vehicle model being investigated. Complexity and

accuracy of CFD simulations are however directly dependent on computer resources and availability of large clusters, which is why steady state realizable k-epsilon simulations are still very common in industry.

Simulating wheels in CFD comes with some simplifications and assumptions which introduce errors into the simulations. These sources can be split into geometrical, solver, and numerical.

The geometrical simplifications are mainly due to limitations in mesh resolution. As tyre pattern details can be quite small, it is very hard to resolve a lot of the details included so some simplification of the geometry is generally accepted. The tyre is usually wrapped in CFD post processing tool in order to de-feature some of the details and build a computationally affordable mesh.

The solver simplifications are mostly based on the solver settings used. One of the most common is the assumption of steady flow and the use of k-epsilon turbulence model. This usually also comes with the implementation of a wall function in order to avoid resolving the boundary layer with an extremely fine mesh.

Numerical errors occur mostly due to difficulties in representing the rotation of the tyre in the simulations. With steady state simulations the rotating parts of the wheel cannot physically move by implementing sliding mesh. It is possible to apply a rotation boundary condition on the different surfaces. However the velocity vector can only be applied tangential to the cell surface. Thus any rotational velocity applied will be projected down on the cell surface. One way to get around that problem is to implement Moving Reference Frame (MRF) on the rotating parts which in turn will give the right velocity on all cell surfaces and has been investigated and used to represent rim rotation (10). The disadvantage in this numerical simplification is that it introduces a numerical error when the flow is not generally along the axis of rotation. This can have a significant effect on the solution. More detailed explanations with test cases are presented below in Section 2.1.

While tyres physically rotate in reality they do not normally do that in CFD due to contact patch deformation. Therefore a rotating wall boundary condition is implemented instead. This study investigates whether current available tools in CFD can substitute sliding mesh approach and present similar outcomes.

2 METHODOLOGY

Rims have been the focus of several numerical investigations where Rotating Wall (RW) boundary conditions, Moving Reference Frame (MRF) and Sliding Mesh (SM) have been investigated (11). In this paper similar investigations will be performed on tyres. This brings a set of complications which did not exist for rim focused simulations. Contact patch area, complexity of the geometry and asymmetric profiles are the largest of these complications. Apart from getting a good representation of the geometry one needs to be able to apply the correct rotational velocity on the tyres. In section 2.1 some approaches and their advantages/disadvantages will be discussed with given examples.

2.1 Rotational boundary conditions

The first and most common way of modelling rotation is using RW. When applying RW it is unfortunately not possible to apply velocities normal to the cell faces. In the case of a wheel for example, this means that all faces which are on the inside of the spokes and all faces which are inside lateral grooves in a tyre pattern will not

be correctly represented. Figure 1 (top left) shows a test case of a solid bar in still air with a rotational velocity applied to the bar. Notice the difference in velocities on the different faces of the bar. One can also see that the cells above the top surface of the bar are not affected. Thus no velocity is introduced into the fluid by applying a rotating wall boundary condition on the top and bottom sides of the bar.

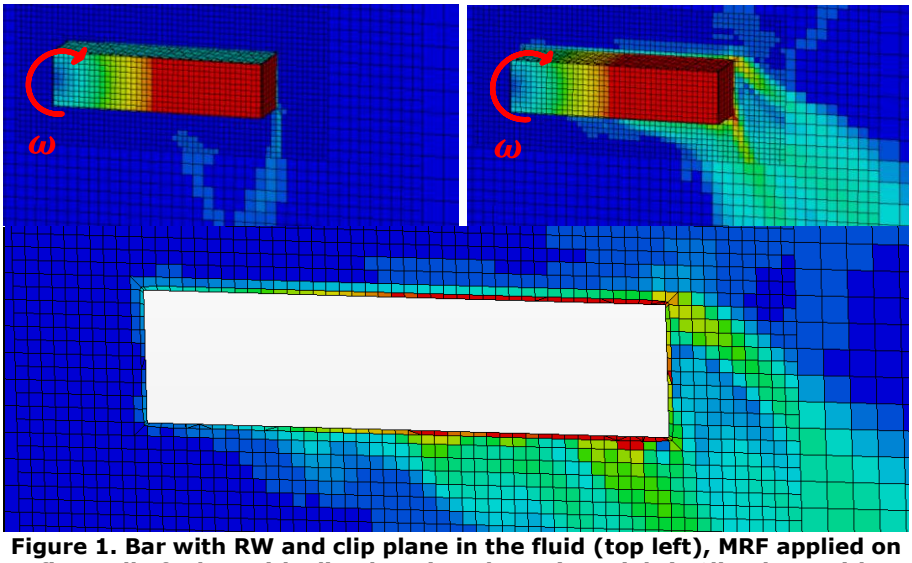

Figure 1. Bar with RW and clip plane in the fluid (top left), MRF applied on first cell of a bar with clip plane in volume (top right), Clip plane with hidden bar for MRF case(bottom); all coloured by velocity from blue to red where blue is zero velocity and red is maximum velocity

MRF is a condition that can be set on a fluid zone which will give all faces in that fluid zone the correct rotational velocity value. It has been widely used in external vehicle aerodynamics simulations on fans and rim spokes in order to simulate the rotating nature of the cells with the assumption that this gives better flow prediction without the expense of unsteady sliding mesh simulations. However the MRF approach does have its drawbacks. The numerical implementation of MRF introduces a pressure gradient into the solution. This mathematical expression for the gradient can be derived by transformation of the rotation from the moving reference frame to the absolute reference frame. This gradient is proportional to the cross product of the cell velocity and set rotation vectors. So for this error to be zero the flow velocity must be aligned with the axis or rotation. In large deviation cases the error can be quite significant. Figure 2 (top) shows a test case of the extreme condition where the flow direction is perpendicular to the axis of rotation. The circle in the centre is an empty air volume with an MRF condition applied to it. The size on the circle is representative of that of a tyre with the applied rotational velocity equivalent to rotation at 100 kph which is the oncoming flow velocity. The mesh in the circle though is not as fine as the one used in the vehicle simulations yet this has been tested in different mesh resolution and the results have shown to be mesh independent. Notice that the pressure gradient introduced, significantly affects the flow velocities with errors going above 40% in velocity due to MRF's inability to preserve uniform flow under these conditions.

However, MRF does indeed give the correct velocity values on the rotating surfaces as seen in figure 1 (top right). The surfaces of the block all get the right boundary conditions when MRF is applied on the first cell surrounding the block. The effect of

MRF is carried out into the fluid from both sides of the bar as seen in the clip plane cut through the volume in figure 1 (bottom).

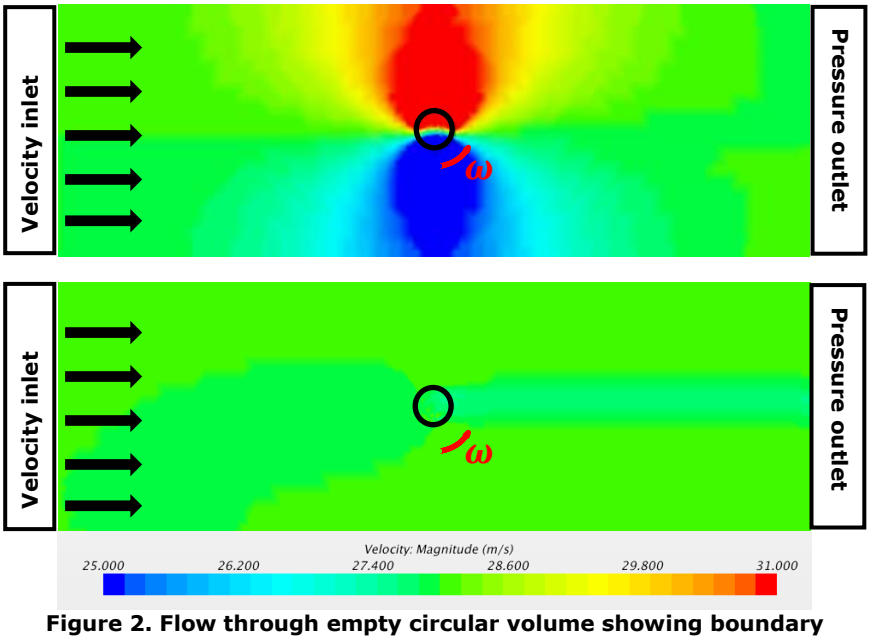

Figure 2. Flow through empty circular volume showing boundary conditions with MRF applied on the circular volume (top) and with SM applied on the circular volume (bottom)

SM is considered as one of the most accurate methods for simulating rotating wheels. As it is a time dependent simulation, the flow will get resolved for different wheel positions. However applications of SM are usually limited to rims as in order to slide the mesh it has to be rotationally symmetric and the tyres are usually deformed at the contact patch due to vehicle loading. However to demonstrate if sliding mesh can preserve uniform flow over its region a small test case, shown in figure 2 (bottom), was run which showed some minor effects introduced into the flow field due to the mesh sliding.

2.2 Numerical setup

Previous work, performed on analysis of tyre aerodynamics, has shown that there are areas to be addressed while performing tyre focused simulations (12). Although trends looked satisfactory, it had to be investigated whether RW could actually give results close to sliding mesh. With that investigation, other methods of applying rotations could be investigated too.

As it is not possible to apply sliding mesh on deformed tyres, for the purpose of this investigation a special set-up has been selected where the vehicle is actually located 10mm above ground with undeformed and unloaded tyres. This also included spacing away the wheel by 10mm from the attachment point on the hubs and simplified disc shaped brake discs have been used for easier meshing inside the rims as seen in figure 3 (left). Also knowing that the flow through the rims interacts significantly with the flow going around the tyres, closed rims where used with flat exteriors. This also helps eliminate the effects of rim spoke position while running sliding mesh simulations. An envelope is generated around the wheel in order to be

able to apply SM around the whole wheel. The sliding mesh volume around the tyre is highlighted in blue in figure 3 (left).

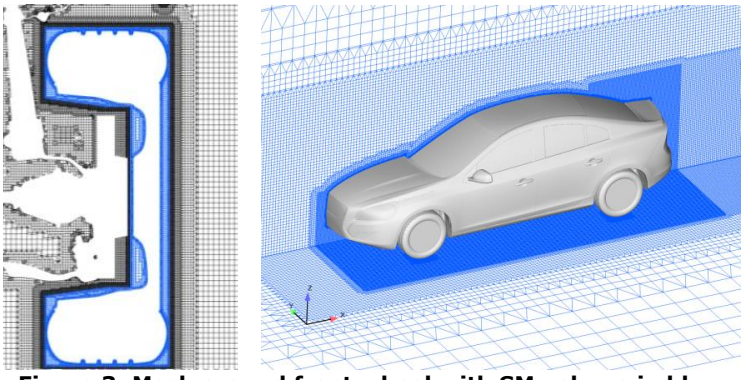

Figure 3. Mesh around front wheel with SM volume in blue

As the main interest is how all of these methods effect the flow field around a vehicle, the test object in all simulations was an S60 car with closed engine compartment. The simulations proved to be very computational expensive thus half car simulations had to be used for all cases. The car geometry and some mesh refinements around the car can be seen in figure 3 (right).

Three different tyres are investigated in the simulations as shown in figure 4. First we have a slick tyre used as reference case referred to as T0 in this paper. Then there are two tyres with detailed tyre patterns referred to as T1 and T2. The tyres were resolved with a target mesh size of 1mm in order to give a reasonable representation of the underlying CAD geometry. Rims were resolved with a 2.5mm mesh size as the level of detail of the geometry was significantly simpler when the rim is flat.

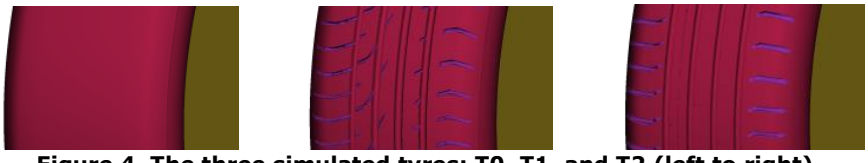

Figure 4. The three simulated tyres: T0, T1, and T2 (left to right)

In order to be able to apply different boundary conditions on the different parts of the tyre it had to be split into different PIDs in ANSA. This meant that the first cell on the tyre tread details can be controlled separately from the rest of the cells on the tyre surface. This helps minimize errors due to MRF in an attempt to correct surface velocities in those details. Shown in figure 4 are the PID splits on the tyre surface. A close zoom into the tyre details will also show how the mesh is built on the tyre in order to have the first cell in the lateral grooves in a separate fluid region. This allows the application of specific boundary conditions. A prism layer of 1mm is built all around the tyre with a 0.5mm layer inside the grooves.

The simulations used Realizable K-Epsilon turbulence model and standard wall function both in the steady and unsteady runs. A few different setups have been investigated. First, all three tyre simulations, were run in steady state with RW and their solution was used as reference and starting point for all later configurations. Then transient simulations were performed with a time step of $2e^{-4}$ s with sliding mesh simulations following straight after.

A new approach to applying rotational velocities has been implemented by combining RW and MRF. Local MRF application has been used to correct for the RW boundary condition thus compensating for lack of velocities inside the pattern grooves. The configuration where MRF is applied only on the pattern grooves is called MRFG and that volume can be seen in red in figure 5. A more extreme configuration where MRF was applied on the first cell of the complete wheel assembly was also performed for comparison and it is given the name MRFG.

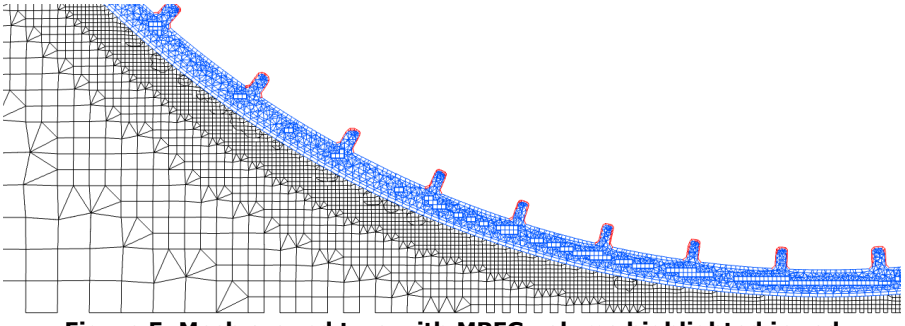

Figure 5. Mesh around tyre with MRFG volume highlighted in red

In an attempt to make the results of the configurations more comparable with the sliding mesh simulations, the RW, MRFG and MRF configurations have also been run in transient mode in addition to the steady state simulations.

3 RESULTS & DISCUSSIONS

3.1 Effects of simulation methods

When running transient simulations no significant changes were noticeable between the transient and steady state simulations. This is expected to be due to the turbulence model being used. Therefore all transient simulations results are not included in this paper and all sliding mesh simulations are compared to the reference steady state simulation directly. Aerodynamic coefficients showed very little fluctuations around the reference values for transient simulations without any sliding mesh.

However when SM simulations were introduced, significant decrease in drag was noticeable for all three types of tyres. Lift values also changed significantly with an increase on all tyres. The drag and lift forces for SM have changed even for the slick tyre which supposedly should have the correct boundary conditions already applied on its surface. This brought up concerns that the size of the sliding volumes is affecting the results. In order to get a better comparison to the effect of sliding mesh from the tyre pattern we will make the assumption that the changes applied to the slick will also happen to the detailed tyres. As the volumes rotating around the tyre are of the same size and similar mesh refinements, then the changes are assumed similar and the values for the sliding mesh simulations will be normalized with the changes on slicks. For this reason, an extra set of bars have been added to the bar charts under the name NSM for Normalized Sliding Mesh configurations although they do not represent a separate set of simulations. The values for NSM have the slick delta between sliding mesh and rotating wall subtracted from the sliding mesh difference of the production tyres to rotating wall. With this assumption the change in coefficients is then attributed to the physical rotation of

the tyre pattern and excluding errors introduced by the volume of choice for sliding mesh.

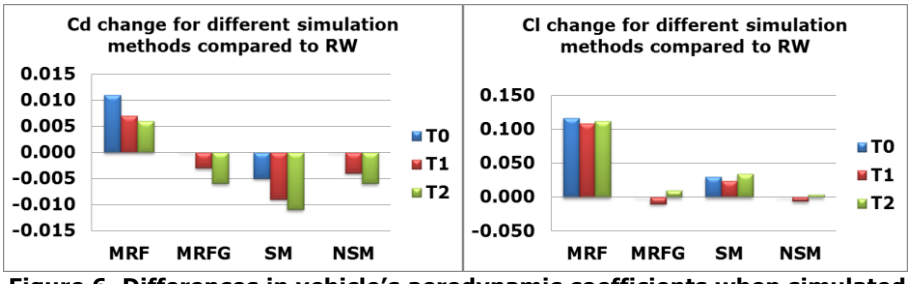

Figure 6. Differences in vehicle's aerodynamic coefficients when simulated with all three tyres using different methods compared to RW

In figure 6, one can see how the aerodynamic coefficients change when we try to apply the different rotation simulation methods. Since the slick tyres have no lateral grooves, the results of MRFG for T0 is the same as RW and this will also be used in the comparison to T0 in figure 7.

The MRF did not deliver a similar trend in drag as SM. MRF drag figures increase significantly. The increase for the slick tyes was significantly higher than for detailed tyres. The lift values have experienced a significant jump which does not look very realistic. This change in lift has been traced back to loss of downforce on the underbody and wheels with an increase in pressure under the car. However it is likely that this increase in lift is due to the numerical error discussed earlier in section 2.1. Even though the MRF boundary condition was only applied on one cell on the surface of the wheel it could still immensely influence the pressure under the vehicle. The velocities around the shoulder of the tyre and below it rise to more than two times free stream velocity. This shows that the velocities in the prism layer around the wheel are very high and lead to a large numerical errors.

For the MRFG case a very similar trend to the one observed for SM can be seen. However after normalizing the sliding mesh simulations in NSM the changes in drag and lift almost match perfectly. One can also note that the trend in drag is opposite to the trend of the MRF case. The MRFG also does not present any of the large lift increases the MRF presents either.

3.2 Effects of tyre pattern design

The Cd and Cl simulated for both detailed tyres were not far apart. This is mainly due to the fact that both tyres have identical profiles and that they are being simulated on a flat rim which will help the flow to stabilize and attach after it goes around the edge of the tyre. Yet there are small differences which are still valuable when showing trends and larger differences when comparing them to the slick tyres. The flow going under the underbody seems to go through less disturbed with the slicks, T0, than it does with T1 and T2 thus resulting in more accelerated flow and lower drag and lift values. T0 presented high downforce values on the front wheels also combined with high underbody downforce. All results showing the lift and drag changes can be seen in figure 7.

In RW cases, T2 and T1 seem to present a noticeable increase in drag and lift compared to T0. One should also note that the T2 presented slightly higher drag while T1 presented slightly higher lift. In MRF case the drag of T1 and T2 seemed to be identical with T1 still showing higher lift than T2. Note that both RW and MRF

failed to predict the results presented by SM where T1 has slightly higher drag than T2 and T2 has slightly higher lift. Also the magnitude of the drag increase in SM for both T1 and T2 was significantly lower than the increase predicted by RW. This puts some question marks on uncertainties in CFD discussed previously about over predicting drag due to tyre details. The fact that some parts of the tread have zero velocities in RW could be one of the reasons contributing to this increase.

The tread velocities have been set using local MRF in MRFG configurations. When running MRFG configuration, and comparing it to the T0 in RW, very similar trends to the SM trends can be seen. Now even T1 is showing higher drag and lower lift that T2. However closer look at the wheel forces have showed that the local forces changes on the wheels when using SM differs from all other combinations tested. This requires further investigation especially to find out where an MRFG configuration compensates for that.

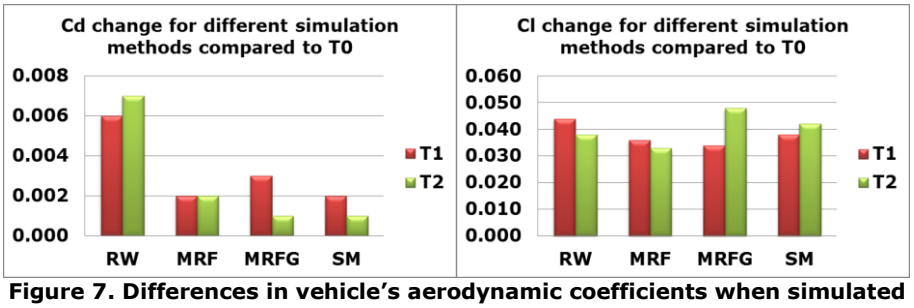

Figure 7. Differences in vehicle's aerodynamic coefficients when simulated with detailed tyres T1 and T2 compared to slick tyre T0

Final note to mention is that since such a method is being developed to be used with loaded tyres which actually have a contact patch, one must be careful when reading these results as things could change when the contact patch is introduced. However as it is not possible to run sliding mesh simulations in that case, then comparison to wind tunnel tests would have to replace that.

4 CONCLUSIONS

There are different methods for applying rotating boundary conditions to wheels yet each has its advantages and disadvantages. It has been seen that comparing detailed tyres to slick tyres can give different results based on the method used. The different ways of applying those methods or the ways they are implemented in the solver can result in various errors that need to be addressed. Even running sliding mesh on a slick tyre with a flat rim still showed some changes in both drag and lift.

As it is very hard to apply sliding mesh on a loaded tyre in CFD simulations a new method has been implemented with the possibility of applying it on steady state simulations. The method is based on a combination of rotating wall and moving reference frame boundary conditions thus allowing it to be applied on non-rotationally symmetric objects. This method has not been tested yet on a loaded tyre though to investigate if any different problems might show up there.

Results of its application, on two production tyres on a flat rim and on an S60 car, have shown to be promising. However, a broader range of tyres and rims still needs to be investigated as the current range of data is not statistically significant yet to judge the effectiveness of the method. A closer look at flow field changes also need to be taken into consideration especially with validation has to be carried out.

5 REFERENCE LIST

1. *The Influence of Ground Simulation and Wheel Rotation on Aerodynamic Drag Optimization - Potential for Reducing Fuel Consumption.* **Wiedermann, J.** 1996. SAE paper No.960672.

2. *On the influence of wheels and tyres on the aerodynamic drag of the vehicles.* **Pfadenhauer, M., Wickern, G. and Zwicker, K.** 1996. MIRA International Conference on Vehicle Aerodynamics.

3. *On the Aerodynamic Interference Due to the Rolling Wheels of Passenger Cars.* **Mercker, E., et al., et al.** Warrendale, PA : s.n., 1991. SAE International (Paper No: 910311).

4. *Drag Reduction Mechanisms Due to Moving Ground and Wheel Rotation in Passenger Cars.* **Elofsson, P. and Bannister, M.** SAE World Congress : s.n., 2002. SAE Paper No. 2002-01-0531.

5. *The Influence of Rotating Wheels on Total Road Load.* **Mayer, Wolfgang and Wiedemann, Jochen.** SAE World Congress : s.n., 2007. SAE Technical Paper 2007-01-1047.

6. **Bonitz, Sabine.** *An investigation into the aerodynamic ventilation drag incurred by wheel rotation on a passenger car, and its influence on the total road load of the car.* Berlin, Germany : Master Thesis, TU Berlin, 2012.

7. *Investigation of Wheel Ventilation-Drag using a Modular Wheel Design Concept.* **Vdovin, A., et al., et al.** 1, 2013, SAE Int. J. Passeng. Cars - Mech. Syst., Vol. 6.
8. *An experimental investigation of wheel design parameters with respect to aerodynamic drag.* **Landström, C., et al., et al.** Stuttgart, Germany : s.n., 2011. FKFS Conference.

9. *Aerodynamic Effects of Different Tire Models on a Sedan Type Passenger Car.* **Landstrom, C., et al., et al.** 1, 2012, SAE Int. J. Passeng. Cars - Mech. Syst., Vol. 5, pp. 136-151.

10. *Investigation of the Influence of Tyre Deflection and Tyre Contact Patch on CFD Predictions of Aerodynamic Forces on a Passenger Car.* **Mlinaric, Peter and Sebben, Simone.** Coventry, England : s.n., 2008. MIRA International Conference on Vehicle Aerodynamics.

11. *New Directions in the Optimization of the Flow around Wheels and Wheel Arches.* **Modlinger, Florian, Demuth, Rainer and Adams, Nikolaus.** Coventry, England : s.n., 2008. MIRA International Conference on Vehicle Aerodynamics.

12. *Investigation of the Influence of Tyre Geometry on the Aerodynamics of Passenger Cars.* **Hobeika, T., Sebben, S. and Landstrom, C.** doi:10.4271/2013-01-0955., 2013, SAE Int. J. Passeng. Cars - Mech. Syst., Vol. 6(1), pp. 316-325.